

Broadband Heating Rate Product Flux Profiles Compared to Clouds and the Earth's Radiant Energy System Radiation Transfer Data Product

*D. Rutan and F. Rose
Analytical Services and Materials Inc.
Hampton, Virginia*

*T. Charlock
National Aeronautics and Space Administration-Langley Research Center
Hampton, Virginia*

*E. Mlawer
Atmospheric and Environmental Research, Inc.
Lexington, Massachusetts*

*T. Shippert
Pacific Northwest National Laboratory
Richland, Washington*

*S. Kato
Hampton University
Hampton, Virginia*

Introduction

The Atmospheric Radiation Measurement (ARM) Program's Broadband Heating Rate Product (BBHRP) is designed to be a standard for validation of radiative heating rates computed by global climate models, cloud resolving models, etc. Inputs for the local scale BBHRP calculations are based on an intensive array of active and passive in situ sensors at the ARM Climate Research Facility (ACRF) Southern Great Plains (SGP) Central Facility (C01). The Clouds and the Earth's Radiant Energy System (CERES), on board the Terra and Aqua spacecraft, produces the Clouds & Radiative Swath (CRS) data product, which is an archive of calculated fluxes at five levels in the atmosphere, produced globally beneath CERES footprints. Inputs for the CRS Surface and Atmosphere Radiation Budget are mainly retrievals based on various passive satellite sensors. To date, validation of the CRS data product has depended on flux observations at the surface (from ARM and other surface observation groups) and at top of atmosphere (TOA) from the CERES broadband instrument. With the advent of BBHRP, it is

possible to make direct comparisons through the atmospheric column. To that end, in this paper one year of CERES/CRS footprint data is collocated in time and space with the SGP Central Facility and resultant match-ups between BBHRP (Version P_i_1.4) and CRS, which are shown with a promising comparison between two independent calculations of flux profiles.

Radiation Transfer Models

At the heart of both the BBHRP and CRS data products are the radiation transfer models, calculating longwave (LW) and shortwave (SW) fluxes. The model used in CRS processing is a modified version of the Fu and Liou (1993) code. It is a delta-two stream (2 for SW, 2/4 for LW) radiation transfer code with 15 spectral bands from 0.175 to 4.0 μm in SW and 12 LW spectral bands between 2850 and 0 cm^{-1} . Cloud optical properties within the model for water clouds are based on the parameterization of Hu and Stamnes (1993), while ice cloud optical properties are from Fu (1996) and Fu et al. (1998) for SW and LW, respectively. Analyzing Moderate Resolution Imaging Spectrometer (MODIS) imager pixels collocated within the larger CERES footprints derives cloud properties input into the model. (Minnis et al. 2003, 2004) Aerosol optical depths are input from the MODIS (MOD08D3) product. The Collins/Rasch Model of Atmospheric Transport and CHemistry (MATCH) model defines aerosol constituents (Collins et al. 2001) and scale heights. Aerosol optical depths from MATCH are used where the MODIS product is unavailable. Actual aerosol properties (single-scatter albedo, scattering coefficient etc.) are given by matching seven aerosol types from MATCH to aerosol properties given by Hess et al. (1998) and Andy Lacis (2004, personal communication). Pressure, temperature, and water vapor profiles are specified from Goddard Earth Observing System (GEOS)-4.0 (a 1-degree gridded reanalysis data product from Goddard Modeling Assimilation Office) and ozone from the National Center for Environmental Prediction, Stratospheric Monitoring Group Ozone Blended Analysis product. Surface albedo comes from a number of different sources. Surface albedo over ocean is derived from a lookup table based on the Coupled Ocean/Atmosphere Radiation Transfer model of Jin (2002). Over clear-sky land, surface albedo is derived from a TOA to surface parameterization using CERES SW observations. Clear-sky surface albedos are pre-processed for a month saving minimum values in an equal angle, ten-minute resolution grid. This "history" map is used to supply broadband albedo under cloudy footprints. Albedo spectral shape is specified as a function of scene type within the CERES footprint. The model is typically run for every other CERES footprint using up to 36 atmospheric levels. These levels include two near surface "floating" levels and "moveable" cloud boundaries for up to cloud levels. CRS assumes no cloud overlap. The model is then run again after adjusting certain input variables so as to better match the CERES observed LW and SW observations. Adjusted and un-adjusted values are reported on the CRS.

The BBHRP radiation transfer models are the Rapid Radiation Transfer Models (RRTMs) developed by Atmospheric and Environmental Research Inc. The longwave model RRTM_LW (Mlawer et al. 1997) uses 16 bands between 10 - 3250 cm^{-1} accounting for absorption using correlated-k technique for water vapor, carbon dioxide, ozone, nitrous oxide, methane, oxygen, nitrogen, and halocarbons. For shortwave (Mlawer and Clough 1998), scattering is accounted for using discreet ordinates with

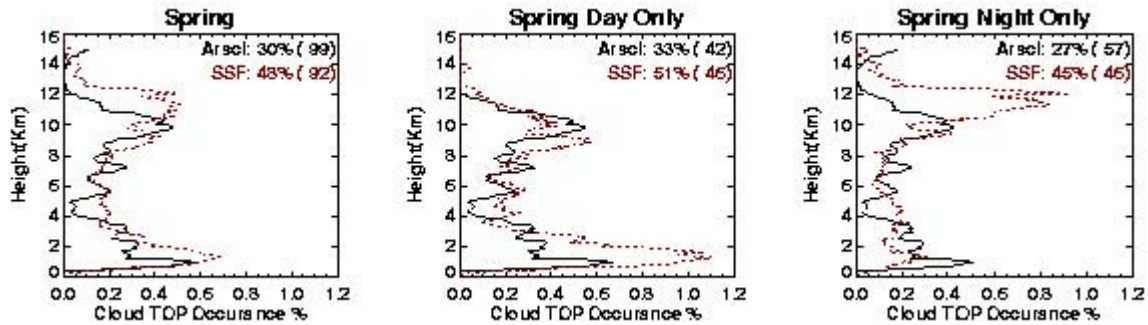
eight streams, in 14 SW bands between 820 - 50000 cm^{-1} . Similar to CRS, cloud optical properties for water clouds are based on Hu and Stamnes (1993), while ice cloud optical properties are from Fu (1996) and Fu et al. (1998). For all cloudy conditions maximum-random cloud overlap is assumed. These models have been extensively validated against line-by-line calculations and results of these comparisons can be found at: http://rtweb.aer.com/rmtm_frame.html. The number of levels specified in BBHRP is a function of the atmosphere and altitude. For clear skies, layers run from 54 m near the surface to 4 km near TOA. The number of levels increases if clouds are present. The atmosphere is specified by radiosonde with column water vapor scaled to microwave radiometer (MWR) measurements. The ozone profile is from the U.S. Standard atmosphere scaled to Total Ozone Mapping Spectrometer. Aerosol optical depths are from the multi-filter rotating shadowband radiometer (MFRSR) with asymmetry parameter given by the ARM Aerosol Observation System for clear skies and all properties by the ARM aerosol best estimate value-added product under cloudy skies. BBHRP results used in this study are Principal Investigator Version 1.4.

Clouds in the Models

Perhaps the most critical input component of the models is the derivation of cloud properties and how they are input into the models. For CRS, cloud properties are determined from MODIS pixels collocated within the larger CERES footprint. MODIS is a passive instrument and properties are inferred from narrowband radiation observations and assumptions regarding the absorption and scattering as measured by MODIS. Each pixel is determined to be clear or cloudy and if cloudy, properties are determined such as phase, optical depth and emitting temperature. These properties are weighted by the energy response function (point spread function) of the CERES observation and included in the CRS data product as distributions over CERES footprints. They represent a real average for a specific time and are input into the model in no more than two levels with an assumption of no overlap. In the case of BBHRP, cloud properties are developed from a suite of instruments at the SGP Central Facility, both active (radar, lidar, ceilometer) and passive (MWR) instruments that are combined in the ARM value added product Active Remote Sensing of Clouds (ARSCL). These data observe clouds in a single column ("pencil" beam) at C01 and cloud properties are averaged over 20 minutes of observation time before being input into the BBHRP routine. Hence, the underlying assumption of how cloud properties are defined and included in the two models, one a spatial average, the other a temporal average at a single place, are fundamentally different. One simple measure of clouds as developed by the two methodologies is to describe their vertical distribution. Figure 1 shows vertical distribution of clouds at C01 over three years (March 2000 through February 2003) as given by the satellite results found on the CRS data product plotted with those from the ARSCL data product. The cloud top distributions (Figure 1a) simply show the altitude the two methods placed cloud tops. Cloud extent shows the percentage over the same time span that a cloud was placed in a particular level in the atmosphere. Overall, the spring comparisons at TOA show remarkably good agreement. However when broken down into day and night one finds a tendency for the satellite to see more high clouds at

night and more low clouds during the day. If we assume the radar estimates a better cloud base, then satellite results indicate a difficulty distributing the clouds low enough into the atmosphere as found in all three plots in Figure 1b.

a) Cloud Top



b) Cloud Extent

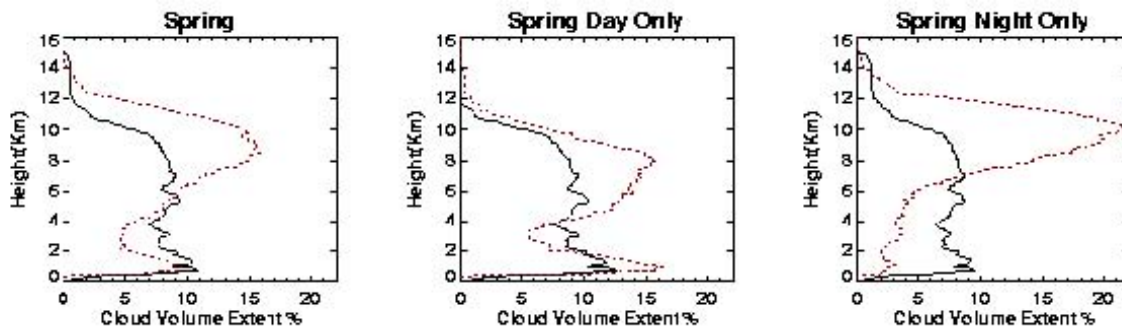


Figure 1. Cloud top a) and extent b) distributions at ARM E13 of both ARSCL (Radar) and CRS (from MODIS pixels collocated within CERES footprints) over three years March 2000 through February 2003, for spring (March, April, and May) subdivided day and night.

Comparison: Model to Model and Model to Observation

Comparisons of skin temperature and surface albedos (mode vs. model) are shown in Figure 2. The relationship between BBHRP and CRS skin temperature (Figure 2a) is quite good with a near zero bias and approximately 1% root mean square (RMS). Recall skin temperatures for BBHRP are derived from upward surface flux at C01 (assuming emissivity of 1) and for CRS they are either from the GEOS4 gridded re-analysis data for cloudy skies, or derived from MODIS radiances for clear skies. Albedo (Figure 2b), on the other hand, does not show such good agreement. CRS albedo is darker than that calculated by BBHRP by 2% absolute or almost 10% relative. For clear sky, the CRS surface albedo is calculated from the CERES TOA flux that covers a much larger area than that observed by downlooking MFRSRs on the C01 tower. Subsequently, it is not expected that these albedos match though more work is needed to quantify why the scaling up of this scene type results in a darker broadband albedo.

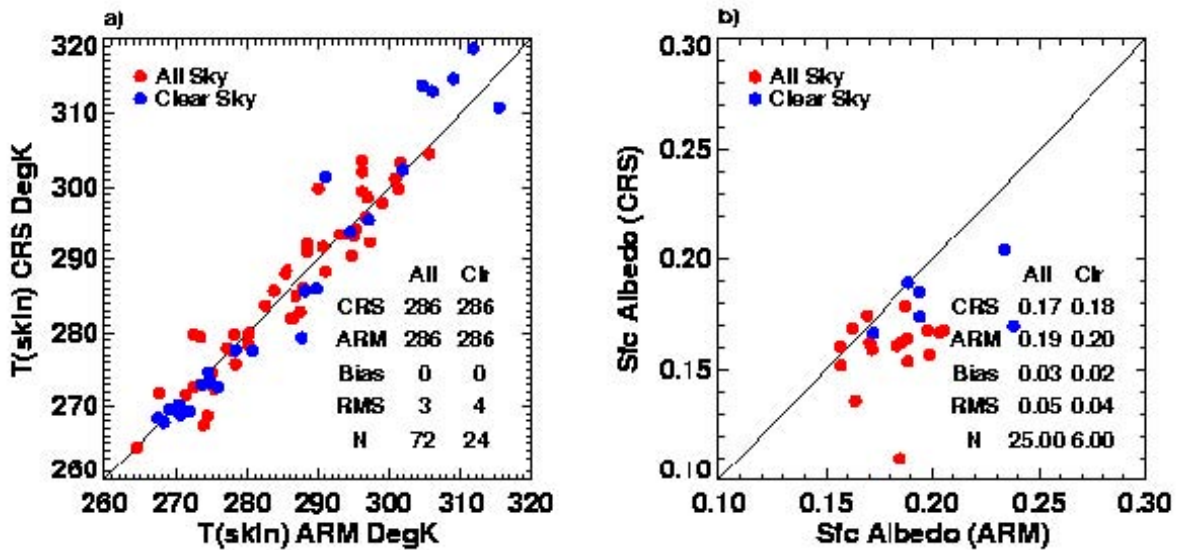


Figure 2. Skin temperature a) and surface albedo b) for BBHRP and CRS model results.

Figure 3 shows a direct comparison of differences (CRS-BBHRP) and variability (1 standard deviation) of model's results at C01. In LW up (Figure 3a), there is an approximately 20 Wm^{-2} standard deviation and less than 5 Wm^{-2} bias at all levels except at the TOA. Above 500 mb, variability remains constant but bias drifts as BBHRP becomes progressively warmer with respect to CRS result with an almost 10 Wm^{-2} bias at the top. LW down (Figure 3b) shows small biases at all levels though increasing variability as the fluxes move downward towards the surface. BBHRP SW upward flux (Figure 3c) is consistently brighter from the surface to TOA than CRS. However, SW down (Figure 3d), which starts at approximately 3 Wm^{-2} greater, BBHRP than CRS, due to a different solar constant, switches sign near the surface with a very large increase in variability with a standard deviation of over 100 Wm^{-2} . This implies that extinction due to clouds or aerosols or both is larger in BBHRP than CRS in the lower atmosphere.

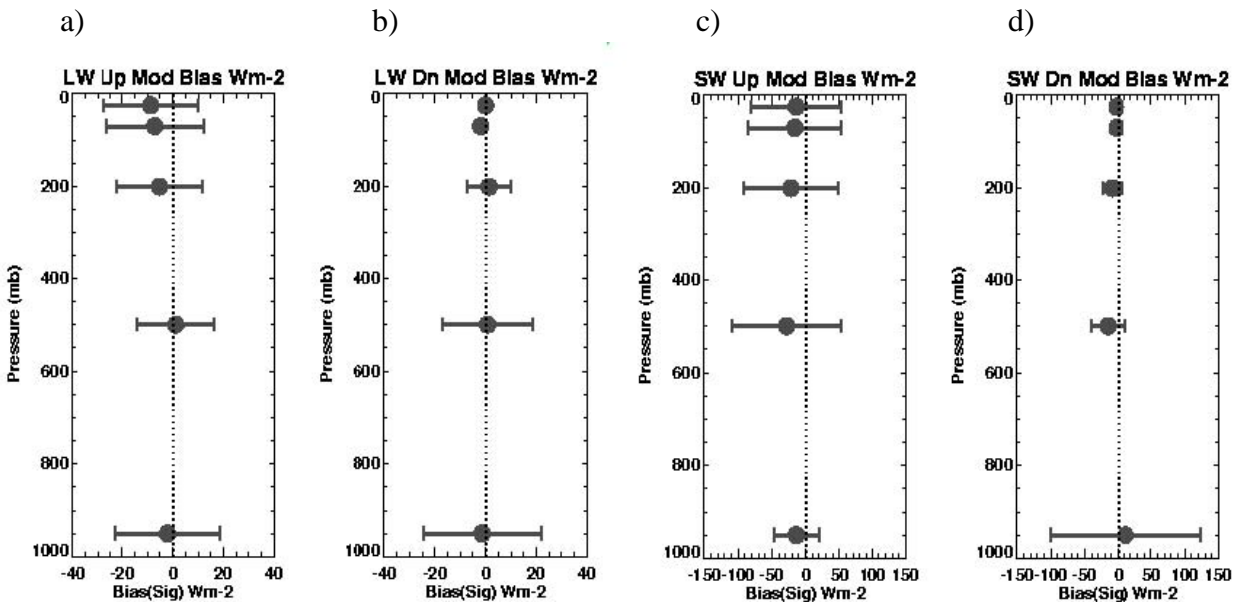


Figure 3. Model to model bias (CRS-BBHRP) and one standard deviation for LW and SW column flux profiles.

Figures 4 and 5 show a series of plots comparing model results, both BBHRP and CRS with flux observations at the TOA and surface. At TOA models are compared to CERES measurements and at the surface results are compared ARM Best Estimate Flux value added product data that has been averaged over 5 minutes. Figures 4a and 4b first show the limited number of daytime matches available for this 12 months worth of data. In fact, because the ARM Enhanced Shortwave Experiment (ARESE) II Intensive Operational Period took place during March 2000, most daytime matches are from that particular month. Nonetheless, both models do reasonably well comparing to CERES SW observations at TOA though CRS results show about one-half the bias and one-third the RMS of BBHRP for all-sky comparisons. For clear skies, both models do well. Though the number of points implies low confidence in our experience, a greater number of comparisons at more surface sites show similar low biases and RMS for clear-sky conditions. The LW results at TOA for CRS are encouraging for both all-sky and clear conditions. BBHRP shows good agreement with CERES at TOA for clear conditions, however the bias (10 Wm^{-2}) and RMS of 21 Wm^{-2} for all-sky suggests potential problems for ARSCL upper-level clouds.

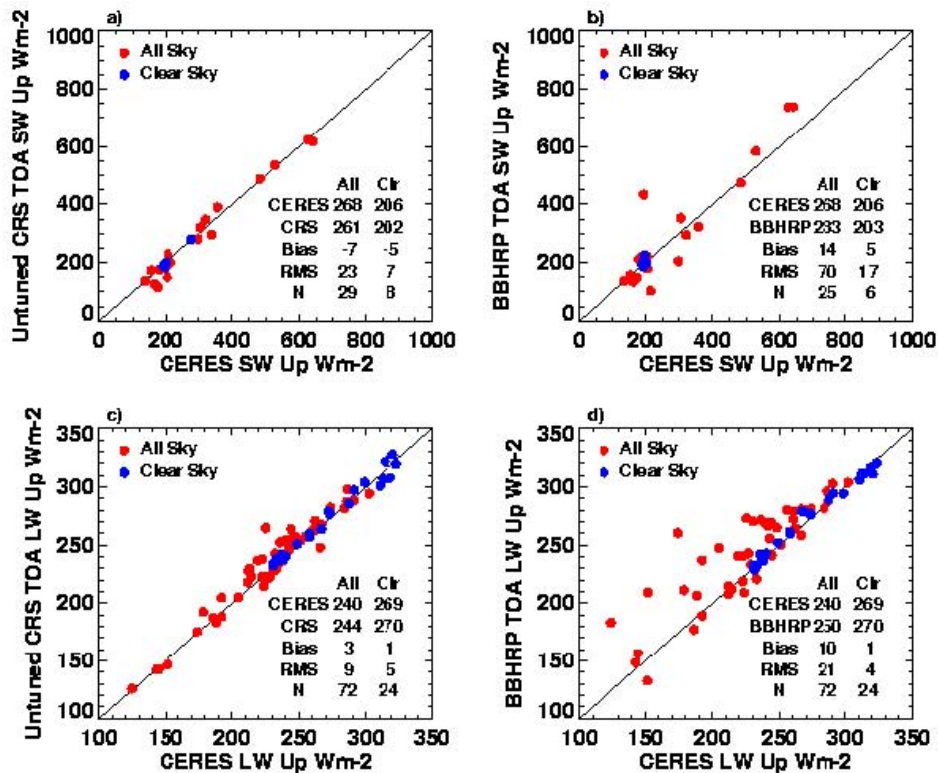


Figure 4. Comparisons of CRS and BBHRP LW and SW fluxes with TOA observations from CERES for a) CRS SW, b) BBHRP SW, c) CRS LW, and d) BBHRP LW.

Figure 5 shows a similar layout of plots but for comparisons of model results to surface observed downward SW and LW flux. Again, for SW statistics, the sample size does not inspire confidence, though both models appear to do reasonably well in terms of bias, RMS is substantial at $100 Wm^{-2}$. This is not unexpected because matching SW model calculations with instantaneous observations almost guarantees large RMS. RMS does drop considerably for both models for clear skies, as expected, though CRS remains more than double that of BBHRP.

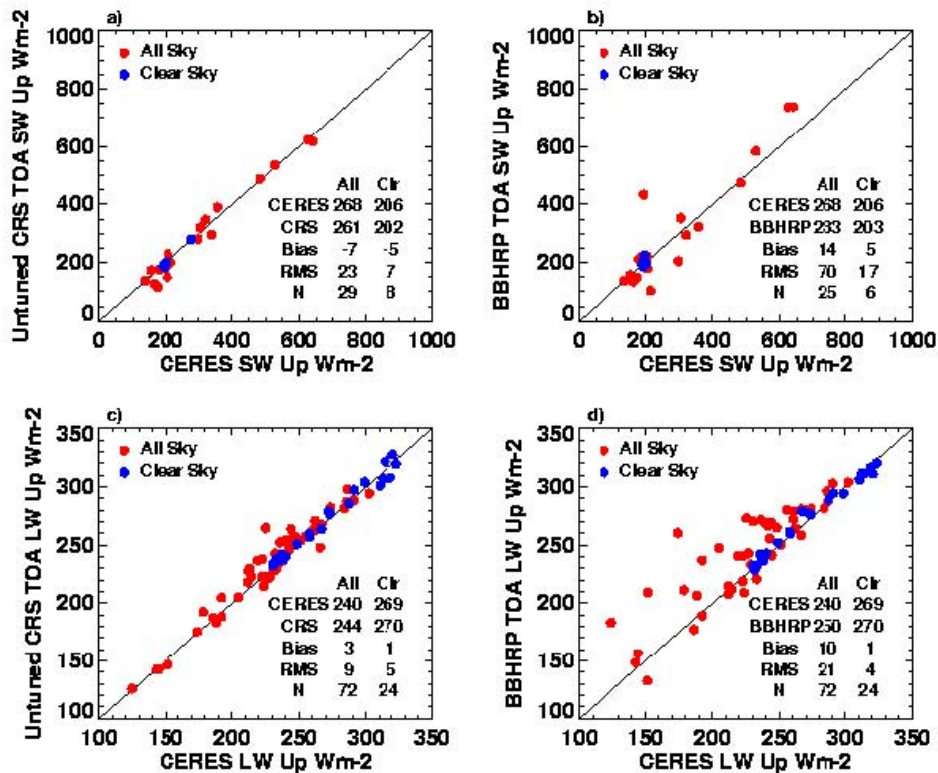


Figure 5. Comparisons of CRS and BBHRP LW and SW fluxes with five-minute averages of surface observations from ARM Best Estimate Surface Flux value added product for a) CRS SW, b) BBHRP SW, c) CRS LW, and d) BBHRP LW.

For LW surface comparison in Figures 5c and 5d, though numbers imply both models are doing equally well, visually one finds that the 15 Wm^{-2} RMS in BBHRP is primarily due to a few outliers whereas RMS for CRS is distributed throughout the time series. This implies that BBHRP is doing better than what the numbers show. Also, from previous studies of CRS surface LW Down there is a known negative bias (-7 Wm^{-2}) due to a near surface air temperature problem in GEOS4 data over the North American continent. Note there is no decrease in bias for clear sky in Figure 5c. However, LW clear-sky bias for BBHRP reduces to about 1% with an RMS of 2%.

Summary

Table 1 summarizes the statistics for model/observation comparisons at TOA and surface as found in Figures 4 and 5. Overall, CRS tends to better match TOA observations, and BBHRP does better at the surface. The large RMS in surface SW with respect to observations is not unexpected though we hope the biases will drop with larger sample sizes. Both models are doing well under clear-sky conditions though BBHRP, with its more sophisticated scattering model and better in situ observations of aerosol, has lower biases and RMS. In the end, however, the comparison of the two products will ultimately come down to a more detailed look at how cloud properties are determined and input into the models.

Figure 1 gives a preliminary look at a bulk characteristic such as vertical distribution. Further study is needed regarding a detailed analysis of the cloud properties. This will have to wait until the daytime sample size is increased. It is currently planned to re-run BBHRP at Terra overpass times, which should greatly increase the number of daytime comparison opportunities.

Table 1. Model biases with respect to observations for LW & SW flux up at the top of atmosphere and LW & SW flux down at the surface.

	Longwave Bias (RMS) (W/m ²)				Shortwave Bias (RMS) (W/m ²)			
	All Sky		Clear Sky		All Sky		Clear Sky	
	BBHRP	CRS	BBHRP	CRS	BBHRP	CRS	BBHRP	CRS
TOA	+10(21)	+3(9)	+1(4)	+1(5)	+14(70)	-7(23)	+5(17)	-5(7)
Surface	-5(15)	-7(18)	-3(7)	-7(11)	-24(86)	-12(79)	+3(11)	-10(27)
N samples	72	72	24	24	25	29	6	8

Acknowledgements

ARM data is made available through the U.S. Department of Energy as part of the Atmospheric Radiation Measurement Program. CERES data is made available from National Aeronautics and Space Administration Langley’s Atmospheric Sciences Data Center at <http://eosweb.larc.nasa.gov/>.

Corresponding Author

David A. Rutan (d.a.rutan@larc.nasa.gov)

References

- Collins, WD, PJ Rasch, BE Eaton, BV Khattatov, J-F Lamarque, and CS Zender. 2001. “Simulating aerosols using a chemical transport model with assimilation of satellite aerosol retrievals Methodology for INDOEX.” *Journal of Geophysical Review* 106:7313-7336.
- Fu, Q. 1996. “An accurate parameterization of the solar radiative properties of cirrus clouds for climate models.” *Journal of Climate* 9:2058-2082.
- Fu, Q, and KN Liou. 1993. “Parameterization of the radiative properties of cirrus clouds.” *Journal of Atmospheric Sciences* 50:2008-2025.
- Fu, Q, P Yang, and WB Sun. 1998. “An accurate parameterization of the infrared radiative properties of cirrus clouds for climate models.” *Journal of Climate* 11(9)2223–2237.
- Hess, MP, P Koepke, and I Schult. 1998. “Optical properties of aerosol and clouds: The software package OPAC.” *Bulletin of the American Meteorological Society* 79:831-844.

Hu, YX, and K Stamnes. 1993. "An accurate parameterization of the radiative properties of water clouds suitable for use in climate models." *Journal of Climate* 6:728-742.

Jin, Z, TP Charlock, and K Rutledge. 2002. "Analysis of broadband solar radiation over the ocean surface at COVE." *Journal of Atmospheric and Oceanic Technology* 19:1585-1601.

Minnis, P, DF Young, S Sun-Mack, PW Heck, DR Doelling, and QZ Trepte. 2003. "CERES cloud property retrievals from imagers on TRMM, Terra, and Aqua." SPIE Tenth International Symposium Remote Sensing, Conference of Remote Sensing Clouds and Atmosphere, Barcelona, Spain, September 8-12, 5235:37-48.

Minnis, P, DF Young, S Sun-Mack, QZ Trepte, RR Brown, S Gibson, and P Heck. 2004. "Diurnal, seasonal, and interannual variations of cloud properties derived for CERES from imager data." In *Proceedings of the Thirteenth American Meteorological Society Conference Satellite Oceanography and Meteorology*, Norfolk, Virginia, September 20-24, CD-ROM, P6.10.

Mlawer, EJ, and SA Clough. 1998. "Shortwave and longwave enhancements in the Rapid Radiative Transfer Model." In *Proceedings of the Seventh Atmospheric Measurement (ARM) Science Team Meeting*, CONF- 970365, pp. 409-413. U.S. Department of Energy.

Mlawer, EJ, SJ Taubman, PD Brown, MJ Iacono, and SA Clough. 1997. "RRTM, a validated correlated-k model for the longwave." *Journal of Geophysical Research* 102:16,663-16,682.

Bibliography

Mlawer, EJ, JS Delamere, SA Clough, MA Miller, KL Johnson, TR Shippert, CN Long, MH Zhang, RA Ferrare, RT Cederwall, RG Ellingson, SC Xie, JA Ogren, and JJ Michalsky. 2004. "Recent developments on the broadband heating rate profile value-added-product." In *Proceedings of the Thirteenth ARM Science Team Meeting*, Broomfield, Colorado.

Kato, S, TP Charlock, and FG Rose. 2005. "Computation of domain-averaged irradiance using satellite-derived cloud properties." *Journal of Atmospheric Oceanic Technology* 22b:146-164.

Rose, FG, and TP Charlock. 2002. "New Fu-Liou code tested with ARM Raman lidar aerosols and CERES in pre-CALIPSO sensitivity study." Presented at the Eleventh Conference on Atmospheric Radiation, Ogden, Utah.

Rutan, DA, FG Rose, N Smith, and TP Charlock. 2001. "Validation data set for CERES Surface and Atmospheric Radiation Budget (SARB)." WCRP GEWEX Newsletter, 11(1)11-12.

Wielicki, BA, BR Barkstrom, EF Harrison, RB Lee, GL Smith, and JE Cooper. 1996. "Clouds and the Earth's Radiant Energy System (CERES): An earth observing system experiment." *Bulletin of the American Meteorological Society* 77:853-868.